

VAEResTL: A Novel Generative Model for Designing Complementarity Determining Region of Antibody for SARS-CoV-2

Saeed Khalilian², Zahra Moti³, Arian Baloochestani⁴, Yeganeh Hallaj⁴, Alireza Chavosh¹ and Zahra Hemmatian^{1,*}

¹MarWell Bio Inc., California, U.S.A.

²Independent Researcher, Iran

³Independent Researcher, The Netherlands

⁴Independent Researcher, Norway

Keywords: Antibody, Nanobody, Complementarity Determining Region (CDR), SARS-CoV-2, COVID-19, Deep Generative Models, Transfer Learning, Bioinformatics, *in-silico* Screening.

Abstract: The global impact of the COVID-19 pandemic underlines the importance of developing a competent machine learning (ML) approach that can rapidly design therapeutics and prophylactics such as antibodies/nanobodies against novel viral infections despite data shortage problems and sequence complexity. Here, we propose a novel end-to-end deep generative model based on convolutional Variational Autoencoder (VAE), Residual Neural Network (Resnet), and Transfer Learning (TL), named VAEResTL that can competently generate CDR-H3 sequences for a novel target lacking sufficient training data. We further demonstrate that our proposed method generates the third complementarity-determining region (CDR) of the heavy chain (CDR-H3) sequences for designing and developing therapeutic antibodies/nanobodies that can bind to different variants of SARS-CoV-2 despite the shortage of SARS-CoV-2 training data. The predicted CDR-H3 sequences are then screened and filtered for their developability parameters namely viscosity, clearance, solubility, stability, and immunogenicity through several *in-silico* steps resulting in a list of highly optimized lead candidates.

1 INTRODUCTION

Antibodies play an important role in therapeutic discovery and vaccine development for a variety of diseases ranging from infectious diseases to cancer and autoimmune diseases (Zohar and Alter, 2020). Wet-lab methods for antibody discovery can be very time-consuming and costly. One of these methods is high throughput screening which is a drug discovery process used to identify the antibody leads that bind to their antigen targets and are within the therapeutics and developability index range (Sharma et al., 2014). The binding site of antibody/nanobody includes a region known as complementarity determining region (CDR) (Murphy et al., 2008). Amongst CDRs, CDR-H3 on the heavy chain is the most variable CDR and typically contributes the most to antigen specificity for antibodies and nanobodies (Tsuchiya and Mizuguchi, 2016). The current COVID-19 pandemic underlines the importance of developing approaches capable of rapidly designing and developing therapeutics and prophylactics against

novel viral infections. Designing CDR-H3 plays a critical role in antibody/nanobody-based therapeutics. Artificial intelligence (AI) and machine learning (ML) techniques have been recently explored for COVID-19 vaccine development to stop the spread of the virus (Ong et al., 2020); however, rapid development of antibodies and nanobodies which can offer therapeutics and prophylactics benefits is of critical importance.

Recently, biologically plausible deep learning (Yoo et al., 2020), and computational models (Adolf-Bryfogle et al., 2018) have been successfully applied to design and optimize CDR loops using deep sequencing data (Norman et al., 2020). Deep generative models using Variational Autoencoder (VAE) have also been applied in designing proteins (Friedensohn et al., 2020), and in predicting protein structures (Guo et al., 2020). Moreover, deep Residual Neural Network models (Resnet) have also greatly improved protein design and protein structure predictions (Lu et al., 2020), and antibody-epitope classification (Ripoll et al., 2021). Nevertheless, the application of Resnet in antibody/nanobody discov-

*Corresponding author email: zara@marwell.bio

ery has been rarely explored. Existing deep learning and VAE-based approaches are often used in conjunction with large datasets and are incapable of discovering and designing new antibodies/nanobodies when facing data shortage for novel targets such as SARS-CoV-2 and its variants. Transfer learning (TL) techniques succeeded in biomedical image classification and various protein prediction tasks (Heinzinger et al., 2019; Valeri et al., 2020); however, to the best of our knowledge, no study in the literature has empowered the deep generative model of VAE with TL to tackle the lack of training data in antibody/nanobody discovery. Here, we leverage the power of deep learning algorithms to predict therapeutic antibodies with binding ability to SARS-CoV-2. We present a novel end-to-end generative "VAEResTL" model to discover amino acid sequences against novel target antigens that lack training data. Our proposed VAEResTL model is based on a VAE model, a Resnet structure, and a Network-based TL technique. We demonstrate Resnet improved our deep generative model VAERes's performance efficiently while providing a deep neural network capable of learning CDR-H3 sequence complexity. The learning from our VAERes pre-trained on sufficient antibody amino acid CDR-H3 sequences on different target antigens can be efficiently transferred for predicting antibody/nanobody amino acid sequences with binding ability to SARS-CoV-2. The VAEResTL predicted CDR-H3 sequences were then subject to *in-silico* screening and filtering for developability parameters namely viscosity, clearance, solubility, stability, and immunogenicity, resulting in potential lead antibody/nanobody CDR-H3 sequence candidates with optimal therapeutic properties.

2 METHODOLOGY

2.1 Datasets and Data Pre-processing

We used amino acid sequences of antibody CDR-H3 derived from deep sequencing data to develop and train our proposed methods. We filtered out CDR-H3 sequences based on their binding ability to SARS-CoV-2 (Raybould et al., 2021) resulting in 2298 sequences which we used as our primary training data. For our TL method, we used three large datasets of three different antigenic targets with a wide variety of antibodies, including ranibizumab (Rani) (the size of the dataset is 67769 sequences) (Liu et al., 2020), yeast display scFv (Yeast) (the size of the dataset is 11038 sequences) (Adams et al., 2016), and chicken ovalbumin (OVA) (the size of the dataset is 65638 se-

quences) (Goldstein et al., 2019) to pre-train our algorithms.

We converted amino acid sequences into a 2-dimensional matrix through one-hot encoding. To have the sequences of various lengths of 8-20 with the fixed lengths of 20, we used padding and added null character J to the left and right sides of sequences. Since there are 24 amino acids (20 standards, two rare (U, O), one unknown (X), and one null (J)), a CDR-H3 sequence with a length of 20 amino acids results in a 20 x 24 matrix. Each row will consist of a single '1' in the column corresponding to the amino acid in that position, whereby this value for all other columns in that row is equal to '0'.

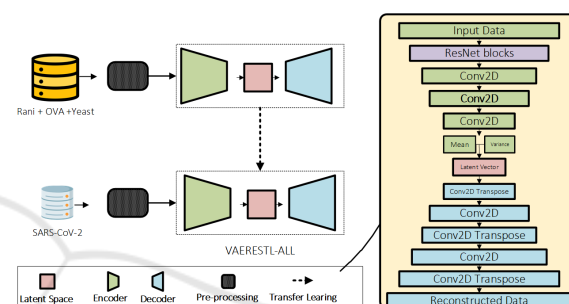


Figure 1: Overview of the proposed method.

2.2 Model Architecture and Training

The VAEResTL, which is an end-to-end trainable model comprises a convolutional VAE that adopts a Resnet structure and is enhanced with a TL technique (Figure 1). Our method utilizes only the amino acid sequences data without the need for structural data. CDR-H3 sequences are subject to high variation in the amino acid distribution and offer the highest contribution to antigen specificity. A deep neural network capable of learning from complex and highly variant sequences is essential to model CDR-H3 sequences; nevertheless, increasing the depth of the neural network by adding more layers leads to a vanishing gradient problem (Goceri, 2019). Resnet introduces skip connections to jump over some layers. The skip connections allow gradients of a deep neural network to flow easily from layer to layer and prevent gradients from vanishing (He et al., 2016). Inspired by the successful applications of Resnet in bioinformatics (Xu et al., 2020), (Ripoll et al., 2021), here we incorporate Resnet blocks into our convolutional VAE model to increase the depth of the neural network for modeling and predicting CDR-H3 sequences. We named our convolutional VAE that adopts a Resnet approach, VAERes. We further incorporated a network-based TL technique (Tan et al., 2018), into our VAERes and named our model VAEResTL (Figure 1).

3 EXPERIMENTS

3.1 Experimental Setup

We executed five experiments and compared VAE, VAERes, VAEResTL with baseline models of HMM and LSTM (Table 1). In experiment 1 and 2, we trained the convolutional VAE and VAERes directly on the SARS-CoV-2 dataset. For our VAEResTL we designed experiment 3, through which VAERes was trained on all the data together including Rani + Yeast + OVA sequences. Then the VAERes pre-trained on Rani+ Yeast+ OVA sequences was trained on SARS-CoV-2 dataset. In experiments 4 and 5, we trained the baseline models of HMM and LSTM directly on the SARS-CoV-2 dataset. HMM and LSTM are based on sequence models described as follows:

- (a) **LSTM**: We adopted an LSTM model previously reported (Gupta et al., 2018), and replaced one-hot encoding with embedding layer. The network consists of two layers of LSTM with 100 units, cross-entropy loss function and Adam optimizer.
- (b) **HMM**: We used HMM model described by Rabiner (Rabiner, 1989) as a character-based model where amino acid characters are considered as states. Each state has a probability distribution over a set of possible sequences. Amino acid characters are then selected to form CDR-H3 sequences.

3.2 Experimental Metrics

We used machine learning (ML) and biophysical metrics to evaluate our proposed methods' performance. We further performed *in-silico* screening to assess the predicted antibody/nanobody CDR-H3 sequences that may bind to SARS-CoV-2.

3.2.1 Sequence Similarity

We used three different metrics to evaluate sequence similarity. **1) Bilingual Evaluation Understudy (BLEU)** (Papineni et al., 2002), We employed 2-gram, 3-gram, and 4-gram to estimate BLEU, using the nltk python library. A higher BLEU score indicates a higher degree of similarity between the seed and the generated sequences. **2) Statistical measures of Jensen-Shannon divergence (JSD)** (Lin, 1991), When the JSD value is close to zero, the distribution of the generated sequences is very close to that of seed sequences. **3) Pairwise sequence similarity method of Needleman-Wunch (NW)** (Needleman and Wunch, 1970) is a biophysical characteristic and is used

to evaluate the sequence similarity between seed and generated sequences (Wang et al., 2020), the higher the NW value, the more similar the two sequences.

3.2.2 Sequence Diversity

We estimated the sequence diversity by measuring the number of shared n-grams for different values of n between generated and seed sequences, referred to as S_n (Das et al., 2018). Therefore, a value of $S_n^{model1}/S_n^{model2} < 1$ implies more diversity of generated sequences by model 1 at a particular n compared to that of model 2.

3.2.3 Biophysical Metrics

We used Bio and modLAMP library (Müller et al., 2017) which incorporates several modules, like descriptor calculation of biophysical characteristics of amino acid CDR-H3 sequences, e.g., stability, isoelectric-point, charge, and hydrophobicity (H) to evaluate the biophysical properties of predicted CDR-H3 sequences (Sharma et al., 2014).

3.2.4 In-Silico Screening

We used the CamSol method, a protein solubility predictor (Sormanni et al., 2015), at pH= 7.0 to estimate the protein solubility score for each CDR-H3 sequence. We measured each sequence variant's net-charge and hydrophobicity (H) (Sharma et al., 2014) to predict the sequences' viscosity and clearance. We predicted the peptide binding affinity of the variant CDR-H3 sequences to MHC Class II molecules to a reference set of 26 human leukocyte antigen (HLA) alleles by employing NetMHCIIpan (Jensen et al., 2018) to reduce their immunogenicity. The NetMHCIIpan' output provides a percentile rank that reflects sequences' affinity compared with a set of random natural peptides. The percentile rank classifies the peptides weak and strong binders to specific MHC Class II alleles. The strong binders have percentile rank of above two, and the weak binders have percentile rank of below ten. The minimum percentile rank, with percentile rank of below ten is also classified as weak binders, and the average percentile rank is calculated across all 26 HLA alleles. The weaker the peptide affinity binding, the less immunogenic is a sequence (Mason et al., 2019).

Table 1: Baseline models comparison. Biological Characteristics and Machine Learning Metrics for generated SARS-CoV-2 CDR-H3 sequences by VAERes, VAEResTL, HMM, LSTM, and Seed SARS-CoV-2.

Method	Biophysical Characteristics					Machine Learning Metrics			
	NW	H	ISO	Charge	Stability	BLEU			JSD
						(2-gram)	(3-gram)	(4-gram)	
VAERes	25.07	0.26	5.08	-2.15	13.18	76.56	75.66	75.59	0.007
VAEResTL	39.31	0.24	5.77	-1.20	25.46	77.57	76.41	75.20	0.005
LSTM	40.51	0.20	4.20	-1.60	57.48	81.12	80.01	78.54	0.11
HMM	9.12	0.52	9.5	0.68	45.9	82.1	80.50	78.60	0.009
Seed	NA	0.23	5.64	-0.84	33.36	NA	NA	NA	NA

4 EXPERIMENTAL RESULTS AND DISCUSSION

4.1 VAE Models Comparison

The convolutional VAE algorithm could not learn the complexity of CDR-H3 sequences, and 100% of the generated amino acid sequences were abnormal (invalid padding or invalid characters) and inappropriate for further analysis. Nevertheless, when we incorporated Resnet structure into the convolutional VAE, our VAERes model demonstrated significant improvements in generating CDR-H3 sequences for SARS-CoV-2. When we trained our VAERes on SARS-CoV-2 seed CDR-H3 sequences, 98% of the generated sequences were valid (valid padding with valid characters), and only 2% of the generated sequences were abnormal (invalid padding or invalid characters). Notwithstanding, 86.8% of the valid generated CDR-H3 sequences for SARS-CoV-2 were duplicate sequences, and only 11.2% of the generated sequences were unique. These results suggest that VAERes could learn a small range of CDR-H3 sequences, reflecting the lack of adequate training data for SARS-CoV-2 seed CDR-H3 sequences as a new target. With VAEResTL, 100% of the generated CDR-H3 sequences for SARS-CoV-2 were valid (valid padding with valid characters), 70.7% of the valid generated sequences were unique, and only 29.3% of the CDR-H3 sequences were duplicate sequences.

4.2 Baseline Models Comparison

When we trained HMM on SARS-CoV-2 seed sequences, HMM could generate a very small library of CDR-H3 sequences which is 1/56 of the size of VAEResTL-generated library of SARS-CoV-2 CDR-H3, where only 17% of the generated sequences were valid (valid padding with valid characters) and

unique. These results may indicate that HMM as a classic model is incapable of learning the complexity of CDR-H3 sequences while suffering from lack of sufficient training data. LSTM could also generate a small library of sequences, where 95.5% of the sequences were valid (valid padding with valid characters). However, 86.1% of the valid generated CDR-H3 sequences for SARS-CoV-2 were duplicate sequences, and only 9.4% of the valid sequences were unique. LSTM could only generate a library of SARS-CoV-2 CDR-H3 sequences which is 1/6 of the size of VAEResTL-generated library of CDR-H3 sequences. We calculated the value for a number of antibody heuristics including Needleman (NW), Hydrophobicity (H), Isoelectric Point (ISO), Charge, and Stability that give biological clues about how VAERes and VAEResTL perform compared to the baseline models of HMM and LSTM (Table 1). The average pairwise sequence similarity of NW is consistently lower for VAERes, and HMM than VAEResTL. Though, the higher NW for LSTM can be due to the bias of such a small ratio of the unique sequences among the small library of valid sequences. The average H value for VAEResTL generated sequences is closer to the seed sequences than generated sequences by VAERes, HMM, and LSTM. The ISO values are between 4.20 and 5.77 across all the other models that are close to the ISO values for the seed sequences, except the HMM generated sequences that has the highest ISO value. The average Charge values for all models are negative except for HMM. The average stability values for VAERes generated sequences are too low. The average stability values for LSTM generated sequences and HMM generated sequences are too high. Therefore, predicted sequences by VAERes, LSTM, and HMM are not appropriate for their biophysical stability property. Moreover, the VAEResTL has a stability value within the range of seed sequences. The overall BLEU values for VAEResTL-generated sequences have higher values for 2-gram, 3-gram, and 4-gram than the BLEU for VAERes. The

small ratio of valid and unique sequences for LSTM and HMM may bias their learning ability to only a small range of CDR-H3 sequences, reflecting the higher BLEU values for LSTM and HMM. Nonetheless, the JSD value for LSTM and HMM is higher than other models presented in Table 1. The overall ML and Biophysical metrics demonstrate VAEResTL can more efficiently predict CDR-H3 sequences with binding ability to SARS-CoV-2. It is likely that with transfer learning, VAEResTL learns a more “biologically plausible” latent space by utilizing a much larger dataset than VAERes and the baseline models of LSTM and HMM. These results may further indicate that VAEResTL architecture loads more biological context during the CDR-H3 sequence generation process. Our baseline model comparison analysis may suggest that VAEResTL outperforms baseline model techniques by predicting a more extensive library of valid and biologically more valuable antibody/nanobody CDR-H3 sequences with binding ability to SARS-CoV-2 more accurately despite the shortage of training data.

4.3 Transfer Learning Impact

Figure 2 compares predicted sequences by VAERes, VAEResTL, with the seed CDR-H3 sequences that bind to SARS-CoV-2 to visually imply the impact of TL. We reported molecular features, e.g., sequence length, amino acid sequence distribution, charge, and H, as they play a crucial role in determining the membrane-binding affinity and specificity. We report the VAEResTL results when our proposed method is pre-trained by Rani + Yeast + OVA. The average amino acid composition-frequency distribution (Figure 2A), length distribution (Figure 2B), net-charge (Figure 2C), and H (Figure 2D) of VAEResTL-generated SARS-CoV-2 CDR-H3 match the seed sequences more than the VAERes-generated SARS-CoV-2 CDR-H3. This observation may suggest that VAERes with TL perform well in capturing the charge patterning, H, and composition within generated sequences.

We further analyzed the diversity of the generated sequences in terms of their shared n-grams (S_n). The n-gram similarity is lower for VAEResTL with respect to VAERes ($S_n^{VAEResTL}/S_n^{VAERes} < 1$) for $n > 2$. 2-gram, 3-gram, 4-gram, 5-gram are 0.91, 0.78, 0.63 and 0.44 respectively. These results imply that VAEResTL-generated sequences show strong long-range diversity; however, they are still consistent with biological sequences, as evident from the sequence similarity comparison (Table 1). The VAEResTL-generated sequences show more substantial diversity

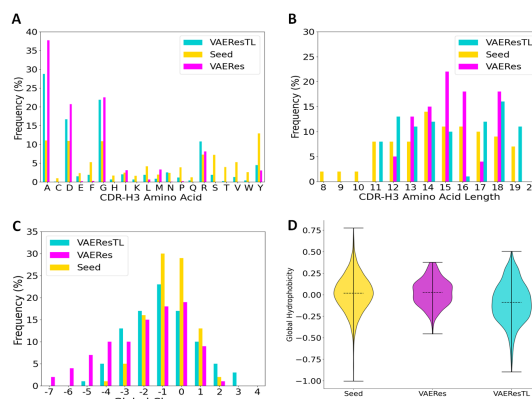


Figure 2: **Visualize Comparison of molecular characteristics** between Seed (SARS-CoV-2 seed sequences, Yellow), VAERes (VAERes-generated sequences for SARS-CoV-2, Violet) and VAEResTL (VAEResTL-generated sequences for SARS-CoV-2, Turquoise). Horizontal dashed lines account for the mean. Whiskers extend to the most extreme non-outlier data points. (A) amino acid distribution, (B) amino acid length distribution, (C) total charge distribution, (D) Eisenberg hydrophobicity.

at higher n-grams (lower S_n values) as a desirable feature that can prevent viral resistance while designing next-generation anti-virals and can provide a larger and more diverse pool of sequences for *in-silico* screening and therapeutics development studies. We also found from the ML visualization heatmaps (Figure 3A1-3C1) and logo plots (Figure 3A2-3C2) that although VAEResTL changed certain CDR-H3 amino acid positions and their frequency distributions, the overall pattern of VAEResTL-generated sequences are closer to seed sequences as compared to the VAERes-generated CDR-H3 sequences. High similarity of predicted CDR-H3 sequences and seed CDR-H3 sequences observed by biophysical and ML analysis may suggest that the VAEResTL-generated CDR-H3 sequences also have binding ability to SARS-CoV-2. Moreover, ML and biophysical characteristics of the VAEResTL-generated CDR-H3 sequences (Table 1, Figure 2, and Figure 3) demonstrate that VAEResTL predicts more biologically valuable CDR-H3 sequences with binding ability to SARS-CoV-2 although, we used diverse training databases. These results show that the generalization for our VAEResTL in antibody/nanobody design is significantly improved.

4.4 In-Silico Screening

With current advances in computational forecasts (Raybould et al., 2019), a number of parameters including viscosity, clearance, solubility, stability, and immunogenicity are used as the guideline for

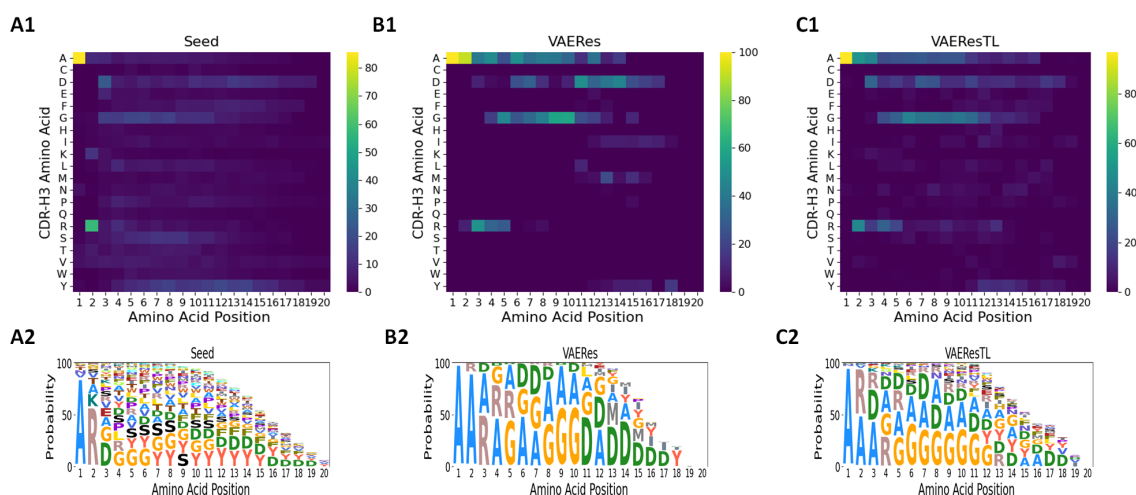


Figure 3: **Visualization of machine learning (ML). Position proposed map.** Heatmap visualization showing: (A1) the count of observed seed sequences for SARS-CoV-2. (B1) the count of VAERes-proposed sequences for SARS-CoV-2 from (left) and to (right) each amino acid at each sequence position. (C1) the count of VAEResTL-proposed sequences for SARS-CoV-2 from (left) and to (right) each amino acid at each sequence position. (seed and VAERes-generated and VAEResTL-generated sequences have the length of 20). *Sequence logo visualizations.* (A2) Sequence logos for Seeds SARS-CoV-2, (B2) VAERes-generated sequences for SARS-CoV-2 (C2) VAEResTL-generated sequences for SARS-CoV-2 are based on residue frequency. Sequence logos are computed using Skylinn.

in-silico screening to select the best in class lead candidates. Although, the predicted sequences are not in clinical stage yet, we characterized the VAEResTL-generated SARS-CoV-2 CDR-H3 sequences compared to seed CDR-H3 sequences on a number of these *in-silico* methods. In order to screen the CDR-H3 sequences' viscosity and clearance we measured net-charge and hydrophobicity (H) by calculating every amino acid sequence of the CDR-H3 sequences. For all the sequences in the library the net-charge is calculated at a given pH=7.0 and the hydrophobicity scale used is "eisenberg" (Müller et al., 2017). The optimal net-charge for drug clearance is between 0-6.2 with H of < 0. Therefore, we filtered out the sequences with a net-charge of < 0 (Figure 4A, marked with red box) and a H of < 0 (Figure 4B, marked with red box). We also calculated the stability of CDR-H3 sequences based on proteins and their dipeptide composition and filtered out sequences with stability values of > 40 and < 20 (Figure 4C, marked with red boxes). We then ran VAEResTL-generated CDR-H3 amino acid sequences through CamSol to estimate their solubility. We filtered out sequences with the CamSol score of < 0.2 (Figure 4D, marked with red box) according to Sormanni et al. (Sormanni and Vendruscolo, 2019) guidelines. The low immunogenicity of antibodies/nanobodies is an essential biophysical property for their therapeutics developability. We predicted the peptide binding affinity of all padded CDR-H3 sequences to MHC Class II by utilizing NetMHCIIpan (Jensen et al., 2018) to reduce

their immunogenicity. We then used peptide's %Rank of predicted affinity that we calculated when comparing CDR-H3 sequences with a set of 200,000 random natural peptides. We predicted affinity for a set of 26 HLA alleles which covers over 98% of the global population. We filtered out the sequences with a %Rank of < 2.5 (figure 4E, marked with red box) (SARS-CoV-2 minimum %Rank) and %Rank of < 70 (Figure 4F, marked with red box) (SARS-CoV-2 average %Rank). After employing *in-silico* screening antibody/nanobody CDR-H3 variants with desired viscosity, clearance, solubility, stability, and immunogenicity remained as potential lead candidates. All remaining predicted CDR-H3 variants against SARS-CoV-2, marked outside the red boxes, confined values equal or superior to the parameters of the SARS-CoV-2 seed sequences. Through the *in-silico* screening, we identified CDR-H3 sequence variants with optimized multi-parameters that can be further evaluated in a wet-lab setting. However, in our future work additional filters, including specificity and humanization, could be implemented to find the most developable therapeutic candidates. In addition, mapping the predicted CDR-H3 sequences *in-silico* on protein/epitope targets can be a valuable validation for our future work.

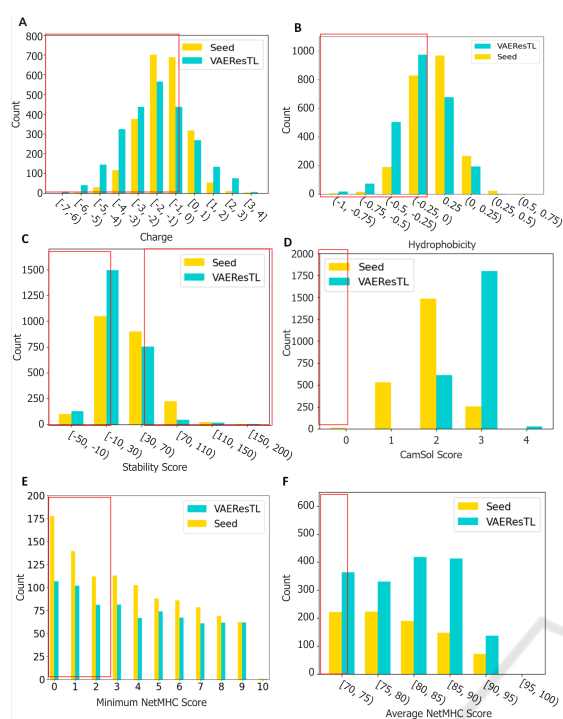


Figure 4: *In-Silico* Screening of predicted CDR-H3 sequences. Histograms present the parameter distributions of generated and seed SARS-CoV-2 sequences for different filtering steps. Red boxes show filtering cut-off for the therapeutic index in clinical setting. (A) CDR-H3 net-charge. (B) CDR-H3 H. (C) CDR-H3 stability score. (D) CamSol solubility score. (E) the minimum NetMHCIIpan %Rank across all possible 15-mers for a given sequence and across all 26 HLA alleles. (F) the average NetMHCIIpan %Rank across all possible 15-mers for a given sequences and across all 26 HLA alleles.

5 CONCLUSIONS

The results of our study exhibit successful application of Resnet adopted VAE for generating novel CDR-H3 sequences. We further illustrate how transfer learning techniques can maximize the power of our VAERes model for antibody/nanobody discovery when dealing with the lack of training data for novel targets such as SARS-CoV-2. Our model was trained on hundreds of thousands of known and diverse CDR-H3 sequences from well-studied targets and created a readily usable tool with extensive generalization capabilities to discover new antibody/nanobodybased therapeutics. To select antibodies/nanobodies with improved characteristics, we identified best lead CDR-H3 sequences with binding ability to SARSCoV- 2 through *in-silico* screening. The outcome of this proof-of-concept study can drive future work for validation of lead candidates through wet-lab experiments and the expansion

of our model for discovery of other CDR fractions to develop therapeutics against different variants of SARS-CoV-2 including Delta and Omicron, as well as other targets. In our future work we will also employ our VAEResTL to design bispecific and trispecific antibodies to develop next generation cancer therapeutics.

ACKNOWLEDGEMENTS

This work was supported by MarWell Bio Inc. No external grants or funding contributed to the completion of this work. All present and future rights to any intellectual property arising from this work will be the sole property of MarWell Bio Inc.

CONFLICT OF INTEREST

The authors declare no conflict of interest.

REFERENCES

- Adams, R. M., Mora, T., Walczak, A. M., and Kinney, J. B. (2016). Measuring the sequence-affinity landscape of antibodies with massively parallel titration curves. *Elife*, 5:e23156.
- Adolf-Bryfogle, J., Kalyuzhnyi, O., Kubitz, M., Weitzner, B. D., Hu, X., Adachi, Y., Schief, W. R., and Dunbrack Jr, R. L. (2018). Rosettaantibodydesign (rabd): A general framework for computational antibody design. *PLoS computational biology*, 14(4):e1006112.
- Das, P., Wadhawan, K., Chang, O., Sercu, T., Santos, C. D., Riemer, M., Chenthamarakshan, V., Padhi, I., and Mojsilovic, A. (2018). Pepcvae: Semi-supervised targeted design of antimicrobial peptide sequences. *arXiv preprint arXiv:1810.07743*.
- Friedensohn, S., Neumeier, D., Khan, T. A., Csepregi, L., Parola, C., de Vries, A. R. G., Erlach, L., Mason, D. M., and Reddy, S. T. (2020). Convergent selection in antibody repertoires is revealed by deep learning. *bioRxiv*.
- Goceri, E. (2019). Analysis of deep networks with residual blocks and different activation functions: classification of skin diseases. In *2019 Ninth international conference on image processing theory, tools and applications (IPTA)*, pages 1–6. IEEE.
- Goldstein, L. D., Chen, Y.-J. J., Wu, J., Chaudhuri, S., Hsiao, Y.-C., Schneider, K., Hoi, K. H., Lin, Z., Guerrero, S., Jaiswal, B. S., et al. (2019). Massively parallel single-cell b-cell receptor sequencing enables rapid discovery of diverse antigen-reactive antibodies. *Communications biology*, 2(1):1–10.

- Guo, X., Tadepalli, S., Zhao, L., and Shehu, A. (2020). Generating tertiary protein structures via an interpretative variational autoencoder. *arXiv preprint arXiv:2004.07119*.
- Gupta, A., Müller, A. T., Huisman, B. J., Fuchs, J. A., Schneider, P., and Schneider, G. (2018). Generative recurrent networks for de novo drug design. *Molecular informatics*, 37(1-2):1700111.
- He, K., Zhang, X., Ren, S., and Sun, J. (2016). Deep residual learning for image recognition. In *Proceedings of the IEEE conference on computer vision and pattern recognition*, pages 770–778.
- Heinzinger, M., Elnaggar, A., Wang, Y., Dallago, C., Nechaev, D., Matthes, F., and Rost, B. (2019). Modeling aspects of the language of life through transfer-learning protein sequences. *BMC bioinformatics*, 20(1):1–17.
- Jensen, K. K., Andreatta, M., Marcotili, P., Buus, S., Greenbaum, J. A., Yan, Z., Sette, A., Peters, B., and Nielsen, M. (2018). Improved methods for predicting peptide binding affinity to mhc class ii molecules. *Immunology*, 154(3):394–406.
- Lin, J. (1991). Divergence measures based on the shannon entropy. *IEEE Transactions on Information theory*, 37(1):145–151.
- Liu, G., Zeng, H., Mueller, J., Carter, B., Wang, Z., Schilz, J., Horny, G., Birnbaum, M. E., Ewert, S., and Gifford, D. K. (2020). Antibody complementarity determining region design using high-capacity machine learning. *Bioinformatics*, 36(7):2126–2133.
- Lu, S., Hong, Q., Wang, B., and Wang, H. (2020). Efficient resnet model to predict protein-protein interactions with gpu computing. *IEEE Access*, 8:127834–127844.
- Mason, D. M., Friedensohn, S., Weber, C. R., Jordi, C., Wagner, B., Meng, S., Gainza, P., Correia, B. E., and Reddy, S. T. (2019). Deep learning enables therapeutic antibody optimization in mammalian cells by deciphering high-dimensional protein sequence space. *BioRxiv*, page 617860.
- Müller, A. T., Gabernet, G., Hiss, J. A., and Schneider, G. (2017). modlamp: Python for antimicrobial peptides. *Bioinformatics*, 33(17):2753–2755.
- Murphy, K., Travers, P., Walport, M., and Janeway, C. (2008). *Janeway's Immunobiology - 7th (Seventh) edition*. Garland Science, New York.
- Needleman, S. B. and Wunsch, C. D. (1970). A general method applicable to the search for similarities in the amino acid sequence of two proteins. *Journal of molecular biology*, 48(3):443–453.
- Norman, R. A., Ambrosetti, F., Bonvin, A. M., Colwell, L. J., Kelm, S., Kumar, S., and Krawczyk, K. (2020). Computational approaches to therapeutic antibody design: established methods and emerging trends. *Briefings in bioinformatics*, 21(5):1549–1567.
- Ong, E., Wong, M. U., Huffman, A., and He, Y. (2020). Covid-19 coronavirus vaccine design using reverse vaccinology and machine learning. *Frontiers in immunology*, 11:1581.
- Papineni, K., Roukos, S., Ward, T., and Zhu, W.-J. (2002). Bleu: a method for automatic evaluation of machine translation. In *Proceedings of the 40th annual meeting of the Association for Computational Linguistics*, pages 311–318.
- Rabiner, L. R. (1989). A tutorial on hidden markov models and selected applications in speech recognition. *Proceedings of the IEEE*, 77(2):257–286.
- Raybould, M. I., Kovaltsuk, A., Marks, C., and Deane, C. M. (2021). Cov-abdab: the coronavirus antibody database. *Bioinformatics*, 37(5):734–735.
- Raybould, M. I., Marks, C., Krawczyk, K., Taddese, B., Nowak, J., Lewis, A. P., Bujotzek, A., Shi, J., and Deane, C. M. (2019). Five computational developability guidelines for therapeutic antibody profiling. *Proceedings of the National Academy of Sciences*, 116(10):4025–4030.
- Ripoll, D. R., Chaudhury, S., and Wallqvist, A. (2021). Using the antibody-antigen binding interface to train image-based deep neural networks for antibody-epitope classification. *PLoS computational biology*, 17(3):e1008864.
- Sharma, V. K., Patapoff, T. W., Kabakoff, B., Pai, S., Hilario, E., Zhang, B., Li, C., Borisov, O., Kelley, R. F., Chorny, I., et al. (2014). In silico selection of therapeutic antibodies for development: viscosity, clearance, and chemical stability. *Proceedings of the National Academy of Sciences*, 111(52):18601–18606.
- Sormanni, P., Aprile, F. A., and Vendruscolo, M. (2015). The camsol method of rational design of protein mutants with enhanced solubility. *Journal of molecular biology*, 427(2):478–490.
- Sormanni, P. and Vendruscolo, M. (2019). Protein solubility predictions using the camsol method in the study of protein homeostasis. *Cold Spring Harbor perspectives in biology*, 11(12):a033845.
- Tan, C., Sun, F., Kong, T., Zhang, W., Yang, C., and Liu, C. (2018). A survey on deep transfer learning. In *International conference on artificial neural networks*, pages 270–279. Springer.
- Tsuchiya, Y. and Mizuguchi, K. (2016). The diversity of h3 loops determines the antigen-binding tendencies of antibody cdr loops. *Protein Science*, 25(4):815–825.
- Valeri, J. A., Collins, K. M., Ramesh, P., Alcantar, M. A., Lepe, B. A., Lu, T. K., and Camacho, D. M. (2020). Sequence-to-function deep learning frameworks for engineered riboregulators. *Nature communications*, 11(1):1–14.
- Wang, Y., Yadav, P., Magar, R., et al. (2020). Bio-informed protein sequence generation for multi-class virus mutation prediction. *bioRxiv*.
- Xu, J., Mcpartlon, M., and Li, J. (2020). Improved protein structure prediction by deep learning irrespective of co-evolution information. *bioRxiv*.
- Yoo, D. K., Lee, S. R., Jung, Y., Han, H., Lee, H. K., Han, J., Kim, S., Chae, J., Ryu, T., and Chung, J. (2020). Machine learning-guided prediction of antigen-reactive in silico clonotypes based on changes in clonal abundance through bio-panning. *Biomolecules*, 10(3):421.
- Zohar, T. and Alter, G. (2020). Dissecting antibody-mediated protection against sars-cov-2. *Nature Reviews Immunology*, 20(7):392–394.